ANL-08/33

MONTE CARLO MODELING AND ANALYSES OF YALINA-BOOSTER SUBCRITICAL ASSEMBLY PART II: PULSED NEUTRON SOURCE

Nuclear Engineering Division

About Argonne National Laboratory

Argonne is a U.S. Department of Energy laboratory managed by UChicago Argonne, LLC under contract DE-AC02-06CH11357. The Laboratory's main facility is outside Chicago, at 9700 South Cass Avenue, Argonne, Illinois 60439. For information about Argonne, see www.anl.gov.

Availability of This Report

This report is available, at no cost, at http://www.osti.gov/bridge. It is also available on paper to the U.S. Department of Energy and its contractors, for a processing fee, from:

U.S. Department of Energy
Office of Scientific and Technical Information
P.O. Box 62
Oak Ridge, TN 37831-0062
phone (865) 576-8401
fax (865) 576-5728
reports@adonis.osti.gov

October 2008 ANL-08/33

MONTE CARLO MODELING AND ANALYSES OF YALINA-BOOSTER SUBCRITICAL ASSEMBLY PART II: PULSED NEUTRON SOURCE

By

Alberto Talamo, Yousry Gohar, and Cristian Rabiti

Nuclear Engineering Division
Argonne National Laboratory
9700 South Cass Avenue
Argonne, IL 60439

Work supported by the
Office of Global Nuclear Material Threat Reduction
U.S. Department of Energy
Under Contract DE-AC02-06CH11357

MONTE CARLO MODELING AND ANALYSES OF YALINA-BOOSTER SUBCRITICAL ASSEMBLY PART II: PULSED NEUTRON SOURCE

Table of Contents

MONTE CARLO MODELING AND ANALYSES OF YALINA-BOOSTER SUBCRITICAL ASSEMBLY PART II: PULSED NEUTRON SOURCE

List of Figures

MONTE CARLO MODELING AND ANALYSES OF YALINA-BOOSTER SUBCRITICAL ASSEMBLY PART II: PULSED NEUTRON SOURCE

List of Tables

MONTE CARLO MODELING AND ANALYSES OF YALINA-BOOSTER SUBCRITICAL ASSEMBLY PART II: PULSED NEUTRON SOURCE

Abstract

One of the most reliable experimental methods for measuring the kinetic parameters of a subcritical assembly is the Sjöstrand method applied to the reaction rate generated from a pulsed neutron source. This study developed a new analytical methodology for characterizing the kinetic parameters of a subcritical assembly using the Sjöstrand method, which allows comparing the analytical and experimental time dependent reaction rates and the reactivity measurements. In this methodology, the reaction rate, detector response, is calculated due to a single neutron pulse using MCNP/MCNPX computer code or any other neutron transport code that explicitly simulates the fission delayed neutrons. The calculation simulates a single neutron pulse over a long time period until the delayed neutron contribution to the reaction is vanished. The obtained reaction rate is superimposed to itself, with respect to the time, to simulate the repeated pulse operation until the asymptotic level of the reaction rate, set by the delayed neutrons, is achieved. The superimposition of the pulse to itself was calculated by a simple C computer program. A parallel version of the C program is used due to the large amount of data being processed, e.g. by the Message Passing Interface (MPI).

The new calculation methodology has shown an excellent agreement with the experimental results available from the YALINA-Booster facility of Belarus. The facility has been driven by a Deuterium-Deuterium or Deuterium-Tritium pulsed neutron source and the (n,p) reaction rate has been experimentally measured by a ^{3}He detector. The MCNP calculation has utilized the weight window and delayed neutron biasing variance reduction techniques since the detector volume is small compared to the assembly volume. Finally, this methodology was used to calculate the IAEA benchmark of the YALINA-Booster experiment.

MONTE CARLO MODELING AND ANALYSES OF YALINA-BOOSTER SUBCRITICAL ASSEMBLY PART II: PULSED NEUTRON SOURCE

1. Introduction

The accelerator driven subcritical assemblies are under consideration for incinerating nuclear waste from nuclear power reactors.[1-3] Consequently, studies and experiments are performed to define their kinetics parameters. The MUSE[4-9] and YALINA[10] are example for such experiments. The MUSE experiments were carried out at the MASURCA facility (Cadarache, France), where a fast subcritical assembly has been driven by an external neutron source from (D-D) or (D-T) reactions. The goals of the MUSE experiments were to validate the computational tools and to investigate methods and techniques for measuring the kinetic parameters of subcritical assemblies. The YALINA-Booster experiments have a similar neutron source driving the subcritical assembly. However, the subcritical assembly has fast and thermal zones with a thermal absorber zone in-between. The coupling between the two zones is only done with fast neutrons. The International Atomic Energy Agency (IAEA) has started two Coordinated Research Projects for accelerator driven systems. The first project is intended to validate computational methods, to characterize the performance of different subcritical systems, and to develop and improve computational and monitoring techniques for the system subcriticality. The second project is for collaborative work on low enriched uranium fuel utilization in accelerator driven systems with the support of the Department of Energy/NNSA's Global Threat Reduction Initiative (GTRI). In this project, the experimental results from the YALINA facility of Belarus are used, including the conversion of the YALINA-Booster to use low enriched uranium instead of the high enriched uranium without changing its performance. The participants of the project are performing computational and experimental benchmark analyses using different computational methods and different nuclear data libraries.

One of the most reliable experimental methods for measuring the kinetic parameters of a subcritical assembly is the Sjöstrand method applied to the reaction rate generated from a pulsed neutron source. The Sjöstrand method requires the time period T (the inverse of frequency) of the neutron source to be much shorter than the delayed neutron precursor half-life (the shortest half-life of the precursor families is 179 ms for ^{235}U) and much longer than the prompt neutron lifetime (~0.1 μs).[11,12] Under these conditions, prompt fission neutrons contribute only to the pulse in which they are generated, whereas delayed neutrons contribute to the pulse in which they are generated and many successive pulses. The delayed neutrons from a specific pulse contribute the for about 200-300 seconds after the pulse since the longest decay half-life of the precursor families is 54.51 seconds for ^{235}U.

At present, the published results for simulating the detector response in a subcritical assembly from a pulsed neutron source neglect the effect of the delayed neutrons from the previous pulses. In the neutron transport simulations of this study, the detector

response is calculated due to a single neutron pulse, so that these simulations cannot predict the detector response due to repeated neutron pulse operation. In the present work, a new computational method was developed to simulate the repeated neutron pulse operation so that the Sjöstrand method measurements can be compared with the computational results as a function of time. The method is based on the simulation of a single pulse over a long time period until the delayed neutron contribution to the detector response is vanished. The obtained detector response is superimposed to itself, with respect to the time, to simulate the repeated pulse operation until the asymptotic level of the reaction rate, set by the delayed neutrons, is achieved. The detector reaction rate due to a single pulse can be easily calculated with great accuracy by the MCNP/MCNPX[13,14] code without any geometry homogenization of the facility. The superimposition of the pulse to itself was calculated by a simple C[15,16] computer program. A parallel version of the C program is required due to the large amount of data being processed, e.g. by the Message Passing Interface (MPI).[17]

This new simulation method correctly predicts the experimental results using the Sjöstrand method and it can be extended to accurately simulate the kinetics measurements using other experimental methods. In fact, this calculational methodology can also be applied to a modulated or random pulsed neutron source with a minor modification of the superimposition program. The pulse superimposition can be done with different frequencies and amplitudes. Consequently, the pulse superimposition method can also validate analytical theories from general reactor physics for evaluating the kinetics parameters.[18-22]

The YALINA-Booster facility includes a fast fuel zone, a thermal fuel zone and a thermal reflector zone; this three zones configuration excludes the application of two-region models for calculating the kinetic parameters.[23] A previous work describes in details the YALINA-Booster facility and its MCNP modeling and analyses.[24] In the kinetics experiments of the YALINA-Booster, the neutron pulse width is 5 or 10 μs and the pulse period is in the range of 8.8 to 20 ms. In the measurement experiments, the (n,p) reaction rate of a ^{3}He detector in the experimental channels was acquired over a 30-minutes period to insure the asymptotic contribution from the delayed neutrons.

2. A Single Pulse Calculation

The YALINA-Booster facility has been modeled in details without any geometrical approximation using the MCNPX computer code as shown in Figures 1 and 2. A complete description of the facility and its Monte Carlo model and analyses can be found in reference 24. In this work, the attention is focused on obtaining an accurate estimate of ^{3}He (n,p) or ^{235}U (n,f) reaction rate in the experimental channels of the YALINA-Booster assembly. The facility has been driven by a pulsed neutron source with a constant period in the range of 8.8 to 20 ms. The neutron source energy is 2.45 or 14.1 MeV. The source neutrons are emitted from the copper disk top surface from a Deuteron-Deuteron (D-D) or Deuteron-Tritium (D-T) reaction, respectively. Once a source neutron is emitted, MCNPX tracks its random walk, including the interaction with the detector material as a function of time. The neutron source is uniformly sampled within the

neutron pulse width and the pulse width is selected in the range of 5-10 μs. MCNPX tallies the ^{3}He (n,p) or ^{235}U (n,f) reaction rate as a function of time in the various experimental channels. The neutrons are tracked for 500 seconds and the 500 seconds interval is divided into 440 intervals with interval width in the range of 10 μs up to a maximum of 10 seconds. For ^{235}U, the longest half life of the delayed neutron precursor families is 54.51 s and this family represents ~3.8% of the total delayed neutrons. The total tallying time is therefore about 10 times the longest half life of the delayed neutron precursor families.

3. Variance Reduction Techniques for a Single Pulse Calculation

Variance reduction techniques were used to improve the statistics of the MCNP tallying results for the delayed neutrons since their fraction is very small relative to the prompt neutrons and the detector volume is much smaller than the facility volume. First, the number of delayed neutrons per fission event was increased and their weights were adjusted (reduced) to track more delayed neutrons. Second the space/time or space/energy weight window capability of MCNP was utilized. This variance technique works for a single tally. MCNP tracks the contribution to this tally from each cell of a superimposed structured spatial mesh to the geometrical model. The superimposed spatial mesh is completely independent of the geometry. The importance of each superimposed mesh cell (I_c) for the selected tally is calculated as follows:

$$I_c = \text{Cell Importance} = \frac{\text{Total contribution to the chosen tally from particles entering the cell including their progenies}}{\text{Total weight of particles entering the cell}}$$

The weight windows were generated in an iterative way to insure that all the phase space (space/time or space/energy) is covered with tracks. During the particle tracking process, MCNPX compares the particle weight relative to the upper/lower bounds of the weight window corresponding to the particle location, and energy or time, to decide the need for splitting or Russian roulette. If splitting or Russian roulette event is considered, the particle weight is adjusted. This weight checking can be performed at each collision and/or surface crossing between two cells of the superimposed spatial mesh. In addition, MCNP can perform a global variance reduction technique based on energy or time over the whole geometrical model. For the same number of source neutrons, the utilization of space weight windows reduces the computation time by a factor of two and it considerably improves the tally statistics for the YALINA-Booster configuration with 1141 fuel rods in the thermal zone. Figure 3 gives an example of the weight windows generated by the MCNP for the ^{3}He (n,p) reaction rate in the EC8R experimental channel.

4. The Pulses Superimposition Methodology

If the nuclear cross sections are not function of the neutron flux, the neutron transport equation is linear. Consequently, the solution of the neutron transport equation

with a repeated pulsed neutron source can be calculated as the superimposition of a single pulse to itself. For continuous pulse operation, the superimposition is repeated until the asymptotic level of the delayed neutrons is reached. This methodology does not require the pulses to have equal frequencies or amplitudes and therefore it can be also applied to a modulated neutron source. Moreover, the superimposition can be either periodically or randomly distributed. The YALINA-Booster facility, as many other research subcritical assemblies, operates at zero power; which maintains the linearity of the transport equation. The cross sections, the material densities, and the geometrical model do not change during the operation.

In the light of the above remark, the reaction rate as a function of time $r(t)$ can be expressed as the sum of the reaction rate $r_n(t)$ given by the nth pulse, as indicated in equation 1.

$$r(t) = \sum_{n=1}^{N} r_n [t - (n-1)T] \qquad (1)$$

In equation 1, T is the pulses period and $r_n(t)$ is independent on n for repeated pulse operation.

A simple C program has been written with the purpose of superimposing the single neutron pulse to itself for 25000 times (pulses) each period of 20 ms. Before superimposing the pulses, a huge array of 50000000 elements (*X*) has been created to have the MCNPX tally results from 0 to 500 s with a constant time interval of 10 μs. The array of 50000000 elements (*X*) has been loaded by the MCNP tally results for a single pulse (array x) according to the following algorithm in C program language:

```
i=0;
time=0;
for (j=0;j<50000001;j++)
   {
   X[j]=x[i];
   time=time+1e-5;
   if (time>=0.9999999999*t[i+1]) i++; }
```

where X represents the huge array of 50000000 elements, x and t represent the reaction rate and time arrays from the MCNPX tally results, respectively (they contain only 440 values), and i, j, and time are scalar variables.

In the MCNP single pulse calculation, the time step was varied to score the details of the tally shape as a function of time. The calculated tally (x) has 440 time step covering 500 s. The single pulse response is almost vanished after the 500 s. The C program has been coupled with the MPI software to reduce the computation time so that 5 processors with a speed of 3 GHz can produce the results in about 15 minutes. Since the huge array *X* requires a large fraction of the RAM memory, few programming techniques are necessary:

- The memory of the huge arrays X and X_{PNS} has to be taken from the C heap instead of the C stack.
- The message passing of the huge arrays X and X_{PNS} in the MPI calls has to be split into several pieces.

Then the following algorithm in C program language is used to superimpose 25000 pulses:

```
for (j=0;j<25000;j++)
i=j*2000
{
for (k=i;k<50000000;k++);
X_PNS[k]=X_PNS[k]+X[k-i];
}
```

where X represents the huge array (50 million units), which is loaded with the single pulse results from MCNPX and X_{PNS} is the huge array (50 million units) containing the superimposition of the single pulse. In the previous algorithm, 2000 is the number of (10 μs) time intervals within a period of 20 ms, so that a period of 20 ms is represented in the X_{PNS} array by 2000 units.

5. YALINA-Booster D-D Experimental Data Comparison with the Analytical Results

The calculated ^{3}He (n,p) reaction rate in the EC6T experimental channel of the thermal zone is plotted in Figure 4 as a function of time due to a single neutron pulse emitted in the YALINA-Booster configuration with 1141 fuel rods. In all the results, the reaction rate has been normalized to its maximum value. The MCNPX simulation was performed with 5 μs neutron pulse width and used the space weight windows variance reduction technique. After about 20 ms from the start of the neutron pulse, the prompt neutrons decayed and the reaction rate diminishes down to the asymptotic level set by the delayed neutrons. Figures 5 to 16 show the reaction rate for some of the 25000 source pulses covering 500 s time period. These plots have been obtained by the C program discussed in the previous section using the MCNPX single pulse results shown in Figure 4. The C program superimposes the initial pulse 25000 times with a constant period of 20 ms. The contribution of the delayed neutrons reaches the asymptotic level after about 5000 pulses (100 s). The asymptotic level is more than 100 times the calculated value of the single pulse. Figure 17 compares the results obtained from a single pulse calculation referred to as MCNP, a single pulse calculation including the delayed neutron contribution from a large number of previous pulses referred to as MCNP/C, and the experimental measurements obtained by a CANBERRA detector with an active length of 25 cm and an active radius of 0.45 cm. These results show an excellent agreement between the numerical simulations and the experimental results. Figure 18 gives similar results for the EC8R experimental channel located in the reflector region for the same configuration. The experimental measurements of Figure 18 were

performed with two different detectors, a 25-cm active length detector (green curve) and a 1-cm active length detector (lavender curve). The detector active radius is 0.45 cm for both detectors. The reaction rates in the EC6T and EC8R experimental channels were simultaneously measured, which reduces the measured experimental values in the EC8R experimental channel. This reduction is due to the fact that the neutrons absorbed in the detector of the EC6T experimental channel do not have the chance to contribute to the neutron flux in the EC8R experimental channel.

Similar results are obtained for YALINA Booster configuration with 902 fuel rods in the thermal zone. The results are given in Figure 19, which are similar to the results of Figure 17 for the YALINA Booster configuration with 1141 fuel rods in the thermal zone. In this comparison the pulse duration is 5 and 10 μs and the pulse period is 20 and 8.8 ms for the 1141 and 902 configurations, respectively. The experimental results have been performed with a CANBERRA detector with an active length of 1 cm and an active radius of 0.45 cm. In the 902 configuration, the asymptotic delayed neutron contribution is smaller than the one of the 1141 configuration. The lower number of fuel rods in the thermal zone reduces the neutron multiplication factor per source neutron for the thermal zone. In the YALINA-Booster, the external neutron source of the thermal zone consists of D-D neutrons and fast neutrons originated from the fast zone. These two components are almost the same for the two YALINA-Booster configurations. The delayed neutron fraction from the fast zone gives a very small contribution to the neutron detector in the experimental channel. In fact, the delayed neutrons have softer energy spectrum relative to the prompt neutrons and therefore the delayed neutrons generated in the fast zone have a higher chance to be absorbed in the boron carbide interface zone which separates the fast and thermal zones. As the number of thermal fuel rods decreases, the fission reaction rates (neutron multiplication) of the thermal zone decreases. This means that the contribution of the source neutrons from the fast zone increases, which results in a lower delayed neutron fraction of the total neutrons contributing to the reaction rate in the EC6T experimental channel of the 902 configuration relative to the corresponding value of the 1141 configuration. This explains the lower asymptotic delayed neutron contribution in the experimental channel shown in Figure 19 relative to Figure 17.

For the 902 configuration, the peak of the prompt neutrons occurs later, relative to the 1141 configuration. Again, the lower neutron multiplication of the thermal zone enhances the contribution of the prompt neutrons from the fast zone entering the thermal zone. However these neutrons spend some time scattering in the fast zone (lead matrix material) before their travel to the experimental channel for direct or indirect contribution. Their contribution is relatively late (tens of μs), which shift the pulse peak as shown in Figure 19. In addition, the pulse duration for the 902 configuration is double relative to the value for the 1141 configuration. This also delays the peak of the prompt neutrons. The blue lines below and above the MCNP/C curve represent the statistical error associated with the MCNPX results with 95% confidence level.

Figure 20 gives the calculated and the experimental results in the EC6T experimental channel for the YALINA-Booster configuration with 1029 fuel rods in the thermal zone. The results are similar to the results of the other two YALINA-Booster configurations shown in Figures 17 and 19. In these experimental measurements the

pulse duration is 10 μs and the pulse period is 13.98 ms. The experimental results have been performed with a CANBERRA detector with an active length of 1 cm and an active radius of 0.45 cm. The MCNPX simulation utilized the space-time weight windows variance reduction technique. As for the 1141 and 902 configurations, the comparison between the numerical results and the experimental measurements shows an excellent agreement.

Table I compares the experimental, MCNP and MCNP/C multiplication factor for different experimental channels and neutron sources. For the 1029 and 1141 configurations, which are close to critical, the agreement between the three sets of values is within few hundreds pcm. For completeness, Table I reports also the source multiplication factor as calculated and discussed in the Part I of this study.[24] All the Monte Carlo simulations for the D-D neutron source explicitly modeled the neutron detector.

6. YALINA-Booster D-T Experimental Data Comparison with the Analytical Results

The ^{3}He reaction rate in the experimental channels EC1B, EC2B, and EC3B for the D-T neutron source with 5 μs width and 20 ms pulse widths are plotted in Figures 21, 22, and 23, respectively. The experimental results used helium-3 detector with 1-cm active length and 0.45 cm active radius. Since these experimental channels are located in the fast zone of the facility, the peak value of the reaction rate occurs at the beginning of the pulse.

The statistical error of the ^{3}He(n,p) reaction rates is relatively higher than the previous results in the experimental channels of the thermal zone. The small value of the ^{3}He(n,p) cross section for fast neutrons results in a very small reaction rate and poor statistical error. The fast zone has a lead matrix material, which does maintain a fast neutron spectrum. As the experimental channels of the fast zone come closer to the thermal zone, the reaction rate increases and the statistical error improve. The very small fraction of the epithermal and thermal neutrons, which stream from the thermal into the fast zone, causes this improvement. Consequently, the results of EC3B experimental channel are much better than the results of EC1B experimental channel, as shown from Figures 21 and 23. In the Monte Carlo simulations for the D-T neutron source, the detector has been explicitly modeled.

7. IAEA Benchmark Calculations

The ^{3}He (n,p) and ^{235}U (n,f) reaction rates in different experimental channels and configuration as defined in the IAEA benchmark specifications[10] were calculated and shown in Figures 24 through 28. The reaction rates were tallied over a cylindrical volume with 20 cm height and a radius equal to the experimental channel radius. For these reaction rates, no significant difference was observed in the results from the D-D and the

D-T neutron sources when the reaction rates are normalized to their peak values. The previous remarks observed for the peak value of the reaction rate as a function of time hold. In this set of MCNP simulations, the detector has not been modeled.

8. Spatial Correction Factors

Table I compares the multiplication factor obtained by the numerical simulations with the multiplication factor obtained by the experimental results. The numerical multiplication factor has been obtained both by MCNP simulations in criticality mode and by MCNP/C simulations in source mode. In the latter case the area method has been applied to the time dependent reaction rate, which provides different multiplication factors depending on the location of the experimental channel.

The experimental multiplication factor has been obtained by the slope fitting method (top rows) and by the area method (bottom rows). For the D-D neutron source, the slope fitting method underestimates the multiplication factor by 200-600 pcm. For the D-T neutron source, no significant difference has been observed between the results obtained by the slope fitting method and those ones obtained by the area method. The multiplication factor depends on the location of the experimental channel also for the experimental results.

In order to compare the numerical and experimental multiplication factor a correction factor has been introduced following the procedure suggested by Bell and Glasstone[26] and applied by Gabrielli et al.[27-28] The correction factor is the ratio between the numerical MCNP k_{eff} (calculated in criticality mode) and the numerical MCNP/C k_{eff} (calculated in source mode) obtained by the area method. When the correction factor is multiplied to the experimental results obtained by the area method, the discrepancy with the MCNP k_{eff} reduces to less than 430 pcm, as shown in Table II. Table III follows the same calculation methodology of Table II and it summarizes the results obtained for the reactivity values. In this case, the correction factor has been calculated as the ratio between the numerical MCNP reactivity (calculated in criticality mode) and the numerical MCNP/C reactivity (calculated in source mode) obtained by the area method. When the correction factor is multiplied to the experimental reactivity, the discrepancy with the MCNP reactivity reduces to less than 15 %, as shown in Table III.

9. Conclusions

This study assessed the YALINA-Booster kinetic performance and the analytical results were compared with experimental results. The comparison shows an excellent agreement. A new calculation methodology has been successfully developed to model the repeated neutron pulse operation for a subcritical assembly. In addition, this methodology can be used to model irregular neutron pulse operation. The methodology is based on performing a single pulse calculation and superimposing the single pulse results by a C code to obtain the performance of the continuous pulse operation. The methodology has been validated by using the MCNPX code, which performs only a

single pulse analysis. The YALINA-Booster assembly with D-D or D-T external neutron source has been analyzed. In the fast experimental channels, the peak reaction rate occurs at the beginning of the pulse. This peak shifts away from the beginning of the pulse in the thermal and the reflector zones. The IAEA benchmark analyses for the YALINA-Booster assembly do not show any significant differences between the reaction rates from D-D and D-T neutron sources.

A spatial correction factor has been used to compare the numerical and the experimental results and to estimate the subcriticality of the YALINA-Booster assembly. The correction factor is the ratio between the MCNP k_{eff} (or reactivity) in criticality mode and the MCNP/C k_{eff} (or reactivity) in source mode calculated by the area method for each experimental channel. When the correction factor is applied, the maximum discrepancy between the numerical and experimental results reduces to less than 430 pcm.

References

[1] C. D. BOWMAN et al., Nuclear Energy Generation and Waste Transmutation Using an Accelerator-Driven Intense Thermal Neutron Source, Nuclear Instruments and Methods in Physics Research A **320**, p. 336, 1992.

[2] C. RUBBIA et al., Experimental Verification of the Concept of Energy Amplification by High Energy Induced Cascade, CERN/ISC, CERN 93-31, 1993.

[3] C. RUBBIA et al., Neutronic Analyses of the TRADE Demonstration Facility, Nuclear Science and Engineering **148**, pp. 103-123, 2004.

[4] S. SOULE et al., Neutronic Studies in Support of Accelerator-Driven Systems: the MUSE Experiments in the MASURCA Facility, Nuclear Science and Engineering **148**, pp. 124-152, 2004.

[5] P. BAETEN et al., Analytical Investigation and Experimental Application of the Source Modulation Technique to Measure ρ/β, Progress in Nuclear Energy **48**, pp 550-558, 2006.

[6] A. BILLEBAUD et al, The MUSE-4 Experiment: Prompt Reactivity and Neutron Spectrum Measurements. Proceedings of the PHYSOR 2002 Conference, Seoul, South Korea, 2002.

[7] A. BILLEBAUD et al., Prompt Multiplication Factor Measurements in Subcritical Systems: from MUSE Experiment to a Demonstration ADS, Progress in Nuclear Energy **49**, pp 142-160, 2007.

[8] Y. RUGAMA et al., Experimental Results from Noise Measurements in a Source Driven Subcritical Fast Reactor, Progress in Nuclear Energy **44**, pp 1-12, 2004.

[9] Y. RUGAMA et al., Preliminary Measurements of the Prompt Neutron decay Constant in MASURCA, Progress in Nuclear Energy **43**, pp 421-428, 2003.

[10] V. BOURNOS et al., YALINA-Booster Benchmark Specifications for the IAEA Coordinated Research Projects on Analytical and Experimental Benchmark Analysis on Accelerator Driven Systems, and Low Enriched Uranium Fuel Utilization in Accelerator Driven Sub-Critical Assembly Systems, IAEA, 2007.

[11] G.R. KEEPIN et al., Delayed Neutrons from Fissionable Isotopes of Uranium, Plutonium and Thorium, Physical Review **107**, pp 1044-1049, 1957.

[12] J.J. DUDERSTADT and L.J. HAMILTON, Nuclear Reactor Analysis. John Wiley & Sons, 1976.

[13] MCNP Team, MCNP5.1.40. LA-UR-05-8617, 2005.

[14] J. S. HENDRICKS et al., MCNPX, VERSION 2.6.B. LA-UR-06-3248, 2006.

[15] B. Kernighan and D. Ritchie, The C Programming Language, Bell Telephone Laboratories, 1978.

[16] P.G. Aitken and B. Jones, Teach Yourself C in 21 Days. Sams Publishing, 1992.

[17] N. Doss et al., A model implementation of MPI. Argonne National Laboratory, MCS-P393-1193, 1993.

[18] P. BAETEN, Heuristic Derivation of the Rossi-Alpha Formula for a Pulsed Neutron Source, Annals of Nuclear Energy **31**, pp 43-53, 2004.

[19] D. BALLESTER et al., On the Applicability of the Pulsing Feynman-Alpha Method: Validation with MUSE Experiments, Annals of Nuclear Energy **32**, pp 1476-1494, 2005.

[20] M. CEDER and I. PAZSIT, Analytical Solution for the Feynman-Alpha Formula for ADS with Pulsed Neutron Sources, Progress in Nuclear Energy **43**, pp 429-436, 2003.
[21] Y. KITAMURA et al., Calculation of the Stochastic Pulsed Rossi-Alpha Formula and its Experimental Verification, Progress in Nuclear Energy **48**, pp 37-50, 2006.
[22] I. PAZSIT et al., Theory and Analysis of the Feynman-Alpha Method for Deterministically and Randomly Pulsed Neutron Sources, Nuclear Science and Engineering **148**, pp 67-78, 2004.
[23] R. KURAMOTO et al., Rossi-Alpha Experiment in the IPEN/MB-01 Research Reactor: Validation of Two-Region Model and Absolute Measurement of β and Λ, Proceedings of the PHYSOR 2006 Conference, Vancouver, Canada, 2006.
[24] A. TALAMO and Y. GOHAR, Monte Carlo Modeling and Analyses of YALINA-Booster Subcritical Assembly, Part I: Analytical Model and Main Neutronics Parameters. Argonne National Laboratory, ANL-NE-08/13, 2008.
[25] T.E. BOOTH, A Sample Problem for Variance Reduction in MCNP, Los Alamos National Laboratory, LA-10363-MS, 1985.
[26] G.I. BELL and S. GLASSTONE. Nuclear Reactor Theory. Van Nostrand-Reinhold, p. 551, 1970.
[27] F. GABRIELLI et al. Accelerator Driven Systems Subcritical Level Monitoring: Evaluation of Spatial Correction Factors for Source-Jerk and Area Methods. Forschungszentrum Karlsruhe, FZKA 720, 2006.
[28] F. GABRIELLI et al. Inferring the Reactivity in Accelerator Driven Systems: Corrective Spatial Factors for Source-Jerk and Area Methods. Progress in Nuclear Energy **50**, pp. 370-376, 2008.

Table I. Neutron multiplication factor of YALINA-Booster calculated by different methods. The used β value is 760 pcm[24] for the experimental results. The experimental multiplication factors on the top rows are obtained by the slope fitting method and those ones on the bottom rows by the area method.

Configuration Neutron Source	**Experimental Channel**	**Experiment Date**	**Experimental k_{eff}**	**MCNPX k_{eff}**	**MCNPX/C k_{eff}**	**MCNPX k_{src}**
902-DD	EC6T	July 2006	0.93401±220 0.93898±220	0.92881±4	0.93983	0.95635
1029-DD	EC6T	July 2006	0.95468±220 0.95978±220	0.95786±7	0.96211	0.97315
1141-DD	EC6T	December 2007	0.97754±110 0.97956±110	0.97972±4	0.97970	0.98683
1141-DD	EC8R		0.97107±140 0.97701±140		0.98049	
1141-DD	EC5T	July 2006	0.97508±220 0.97395±220		-	
1141-DD	EC6T		0.97475±200 0.97956±200		0.97961	
1141-DD	EC7T		0.97395±220 0.97619±220		-	
1141-DT	EC1B	February 2008	0.97280±480 0.97139±480		0.97553	0.99143
1141-DT	EC2B		0.97370±410 0.97286±410		0.97667	
1141-DT	EC3B		0.97620±160 0.97603±160		0.97879	

Table II. Comparison of the experimental (E) and numerical (C) multiplication factors. The correction factor has been calculated as the MCNP k_{eff} (C) obtained in criticality mode divided by the MCNP/C k_{eff} obtained in source mode with the area method.

Configuration Neutron Source	Experimental Channel	Experimental k_{eff}	Correction Factor	Corrected Experimental k_{eff} (E)	MCNP k_{eff} (C)	C/E
902-DD	EC6T	0.93898±220	0.988	0.92797±220	0.92881±4	1.00091
1029-DD	EC6T	0.95978±220	0.996	0.95554±220	0.95786±7	1.00243
1141-DD	EC6T	0.97956±110	1.000	0.97958±110	0.97972±4	1.0014
1141-DD	EC8R	0.97701±140	0.999	0.97624±140	0.97972±4	1.00356
1141-DT	EC1B	0.97139±480	1.004	0.97556±480	0.97972±4	1.00426
1141-DT	EC2B	0.97286±410	1.003	0.97590±410	0.97972±4	1.00392
1141-DT	EC3B	0.97603±160	1.001	0.97696±160	0.97972±4	1.00283

Table III. Comparison of the experimental (E) and numerical (C) reactivity. The correction factor has been calculated as the MCNP reactivity (C) obtained in criticality mode divided the MCNP/C reactivity obtained in source mode (with the area method).

Configuration Neutron Source	Experimental Channel	Experimental ρ [$]	Correction Factor	Corrected Experimental ρ [$] (E)	MCNP ρ [$] (C)	C/E
902-DD	EC6T	-8.55	1.197	-10.24	-10.085	0.98486
1029-DD	EC6T	-5.51	1.117	-6.16	-5.7887	0.93972
1141-DD	EC6T	-2.75	0.999	-2.74	-2.7237	0.99405
1141-DD	EC8R	-3.10	1.040	-3.22	-2.7237	0.84587
1141-DT	EC1B	-3.88	0.825	-3.20	-2.7237	0.85116
1141-DT	EC2B	-3.67	0.867	-3.18	-2.7237	0.85116
1141-DT	EC3B	-3.23	0.955	-3.09	-2.7237	0.88146

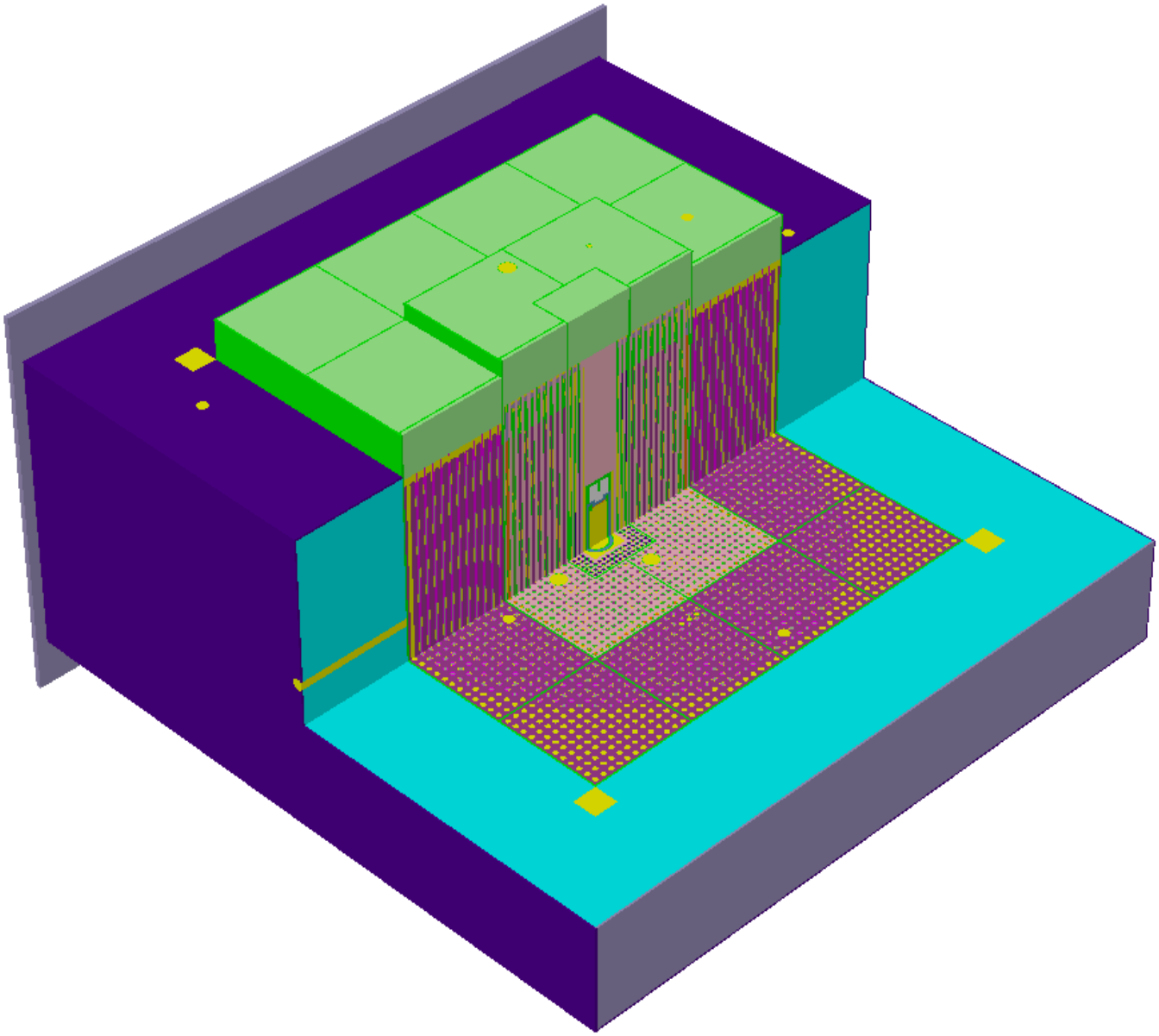

Figure 1. YALINA-Booster Geometrical Model

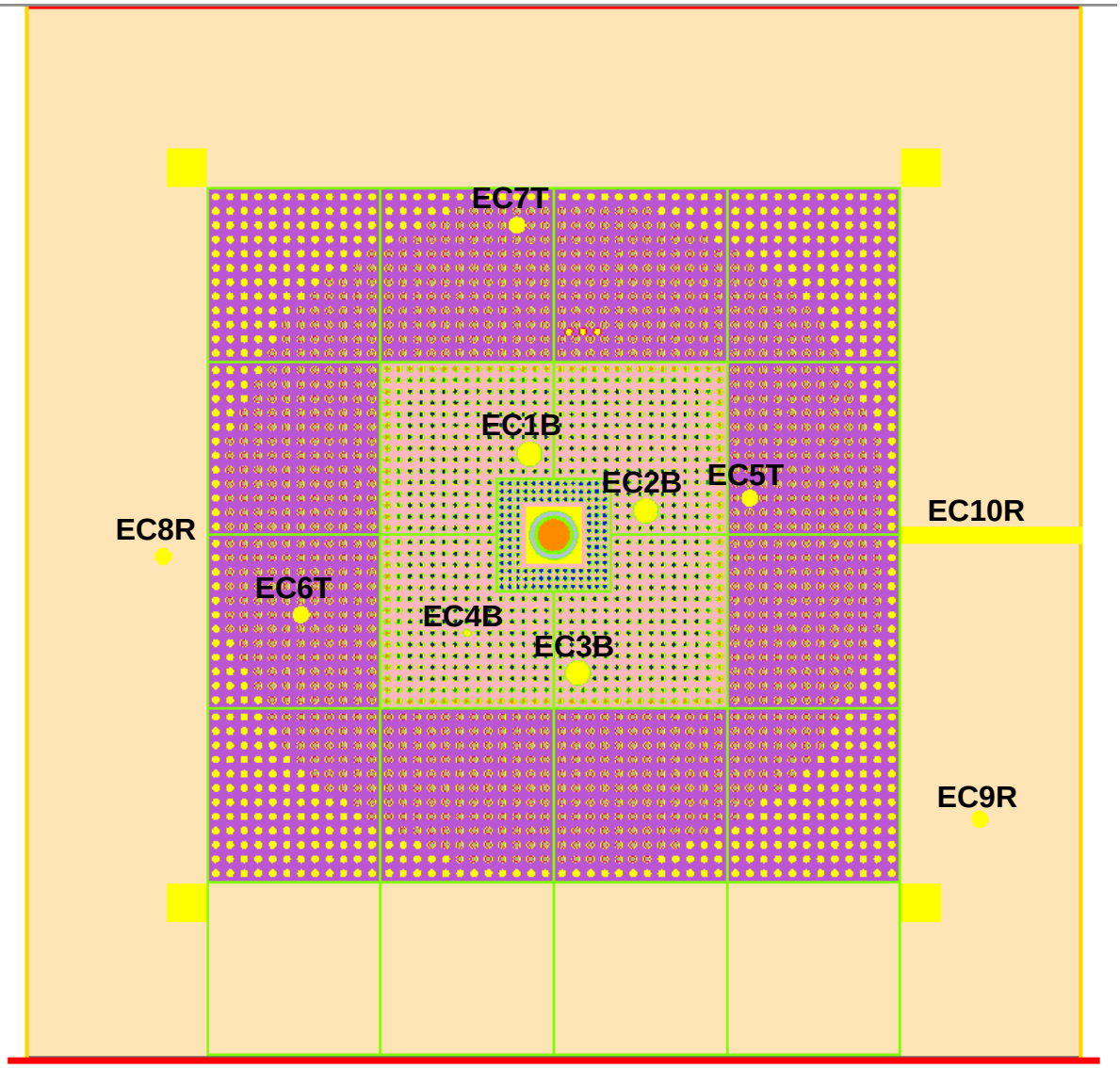

Figure 2. Horizontal section of the YALINA-Booster subcritical configuration with 1141 EK-10 fuel rods

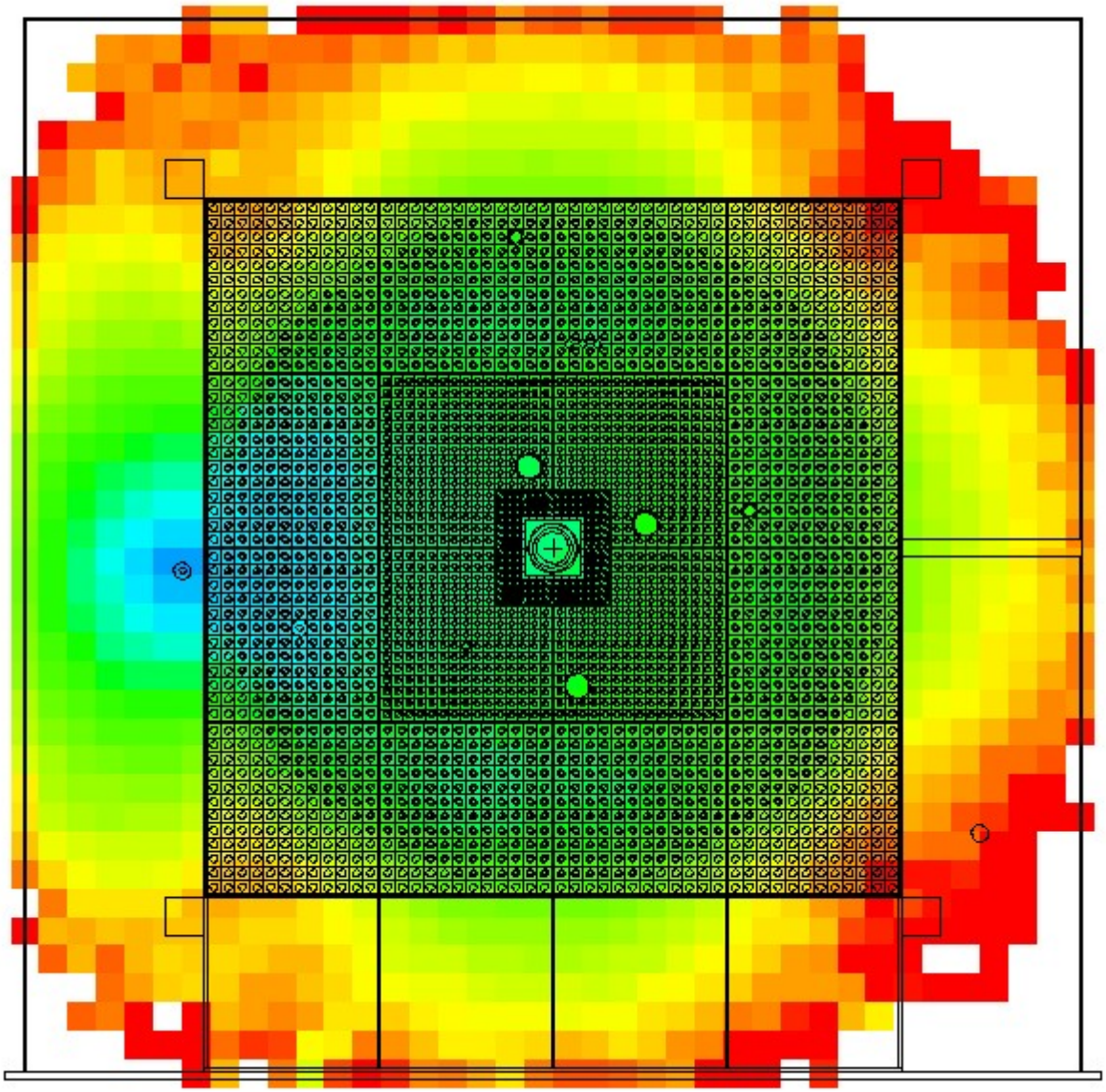

Figure 3. The mesh importance calculated by the weight window generator of MCNP over a spatial mesh superimposed to the Yalina Booster geometry. The scoring detector is in the EC8R experimental channel

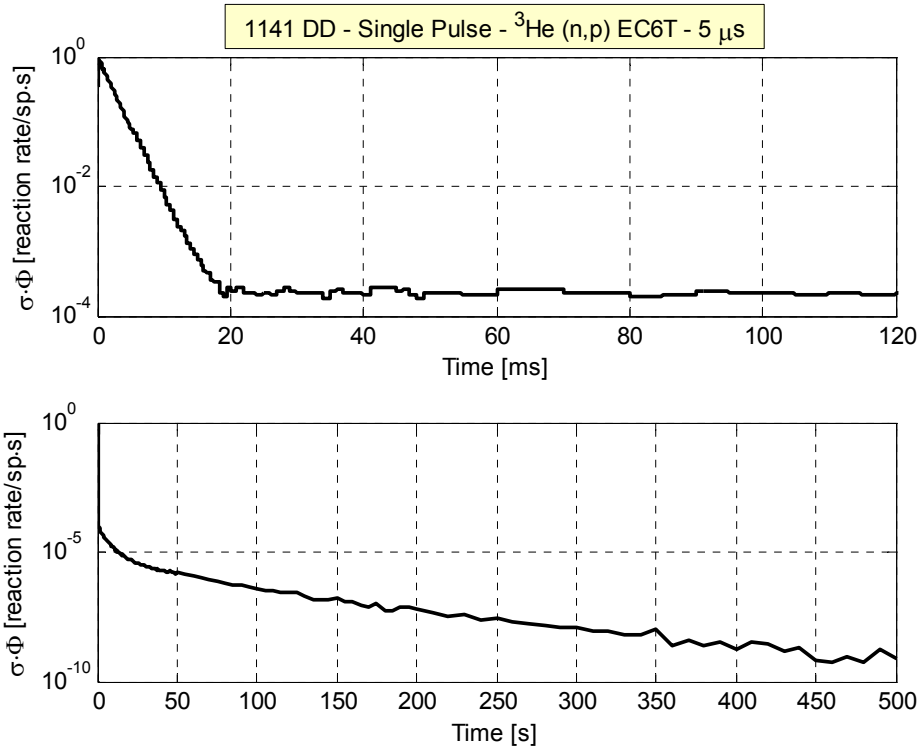

Figure 4. ^{3}He(n,p) reaction rate calculated with MCNPX from a single D-D neutron pulse for the 1141 YALINA-Booster configuration

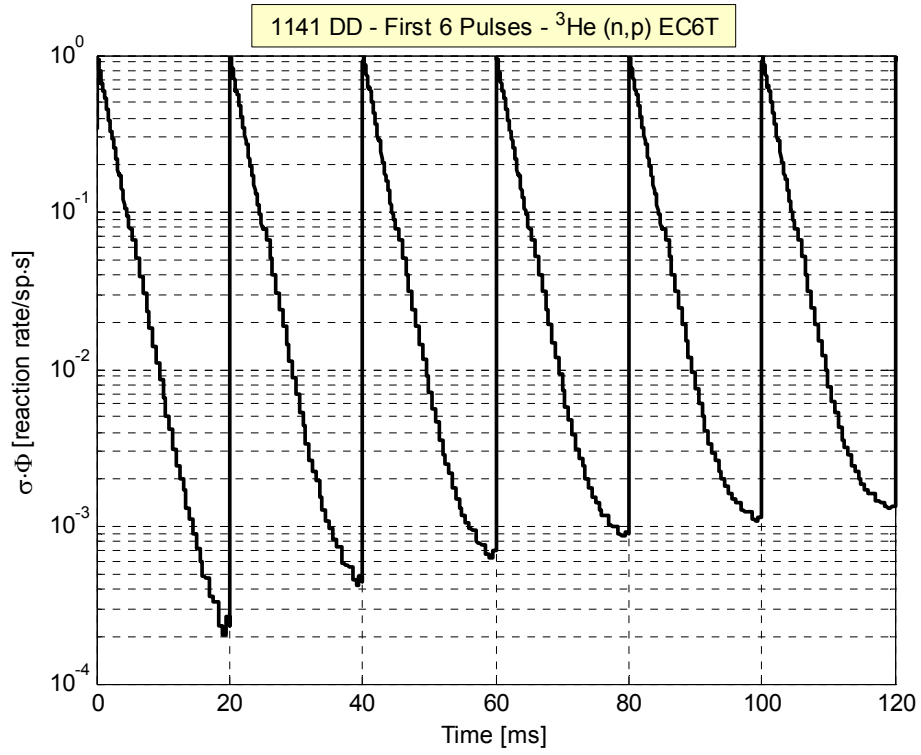

Figure 5. ^{3}He(n,p) reaction rate calculated for the first 6 successive D-D neutron pulses for the 1141 YALINA-Booster configuration

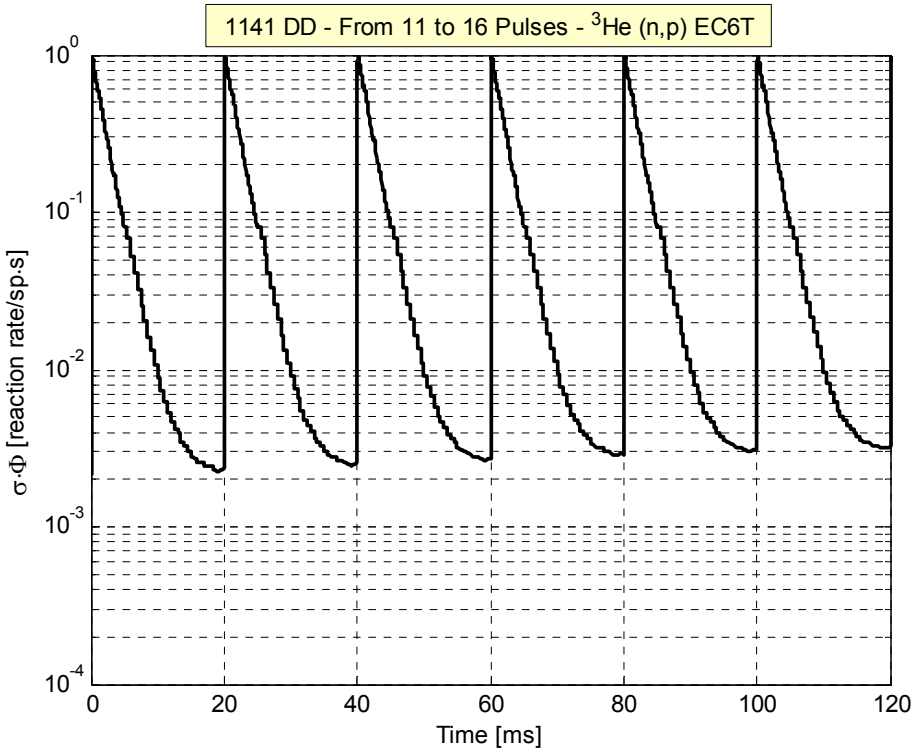

Figure 6. ^{3}He(n,p) reaction rate calculated for 6 successive D-D neutron pulses starting from pulse number 11 for the 1141 YALINA-Booster configuration

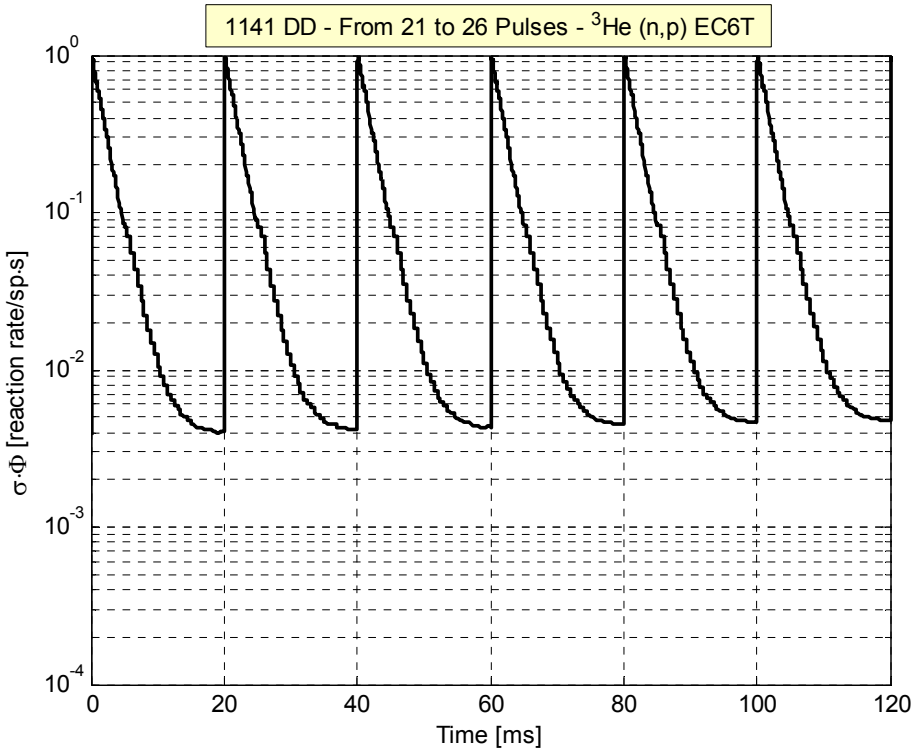

Figure 7. ^{3}He(n,p) reaction rate calculated for 6 successive D-D neutron pulses starting from pulse number 21 for the 1141 YALINA-Booster configuration

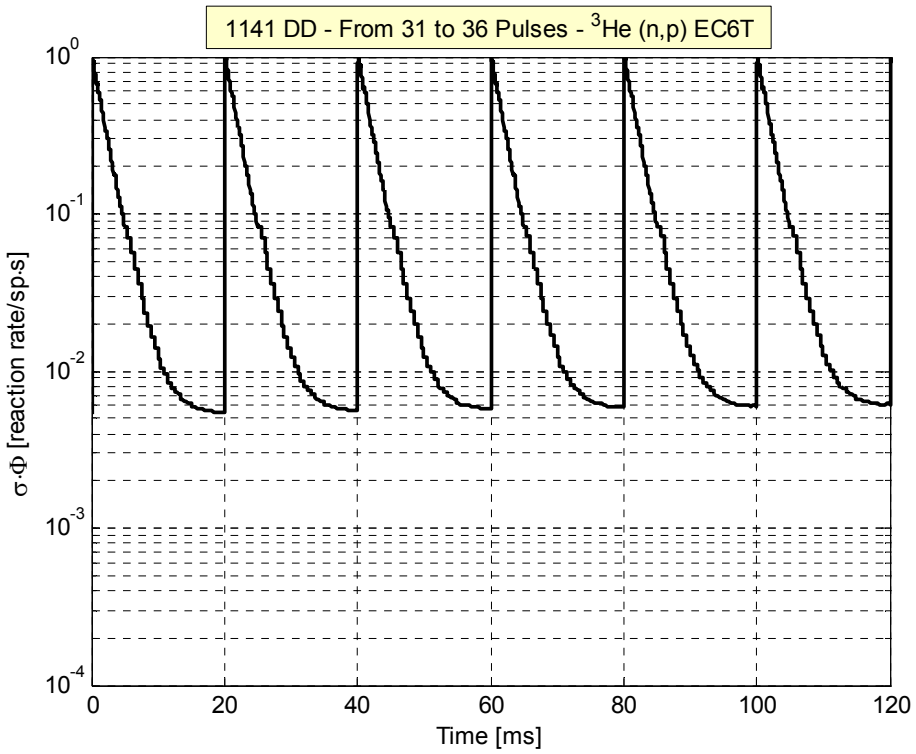

Figure 8. ^{3}He(n,p) reaction rate calculated for 6 successive D-D neutron pulses starting from pulse number 31 for the 1141 YALINA-Booster configuration

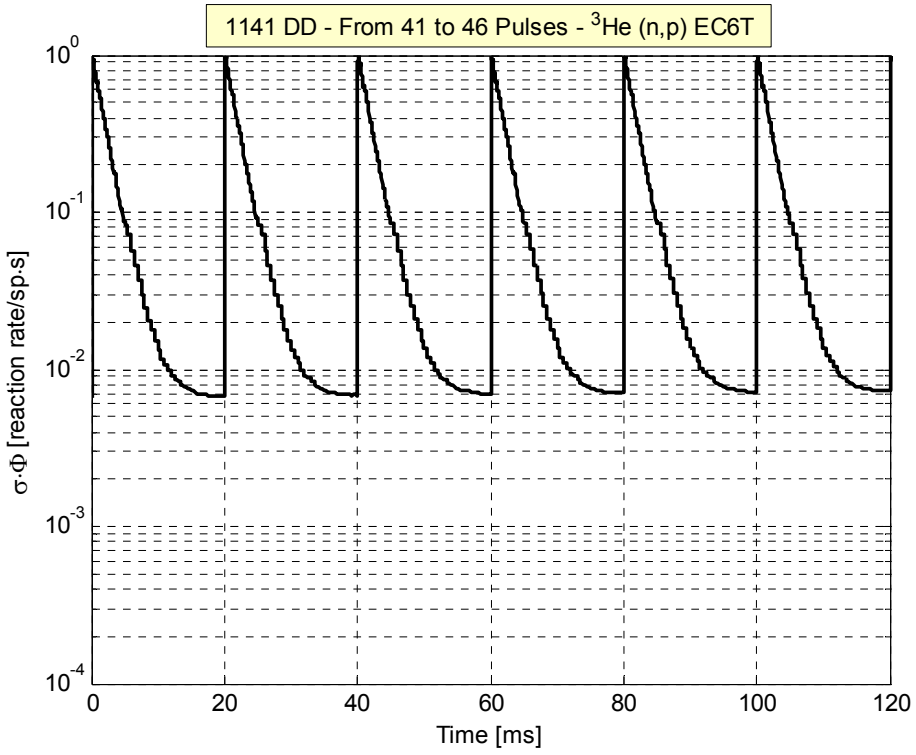

Figure 9. ^{3}He(n,p) reaction rate calculated for 6 successive D-D neutron pulses starting from pulse number 41 for the 1141 YALINA-Booster configuration

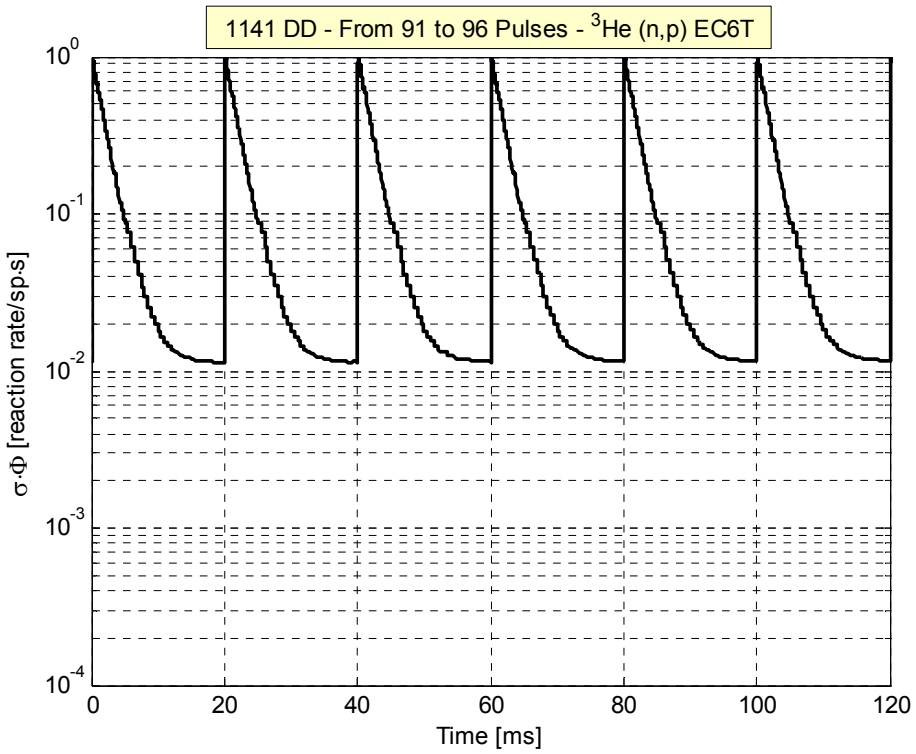

Figure 10. ^{3}He(n,p) reaction rate calculated for 6 successive D-D neutron pulses starting from pulse number 91 for the 1141 YALINA-Booster configuration

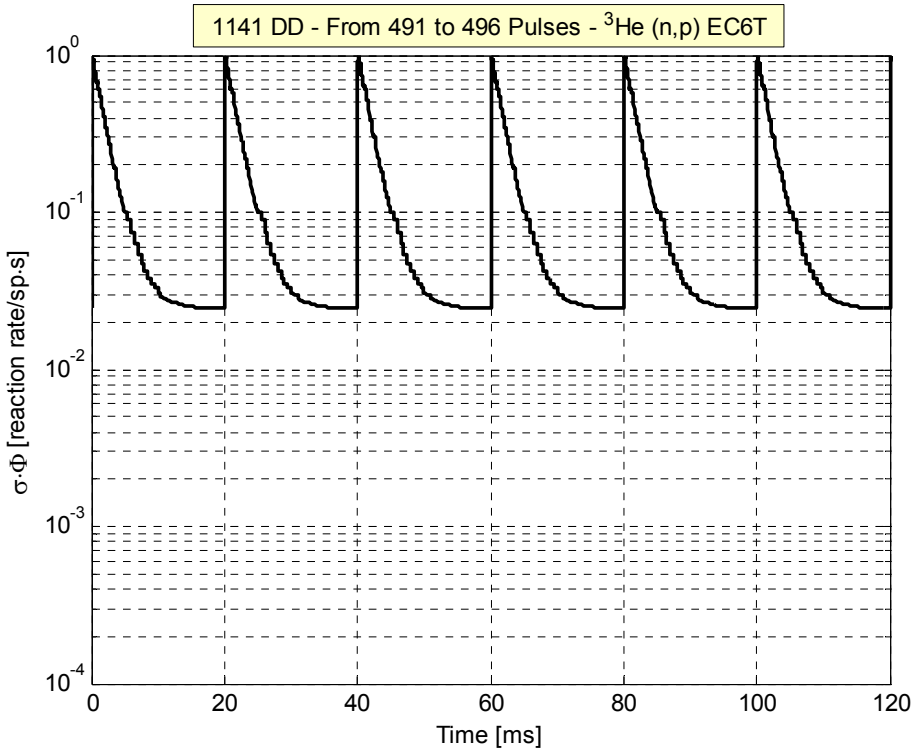

Figure 11. ^{3}He(n,p) reaction rate calculated for 6 successive D-D neutron pulses starting from pulse number 491 for the 1141 YALINA-Booster configuration

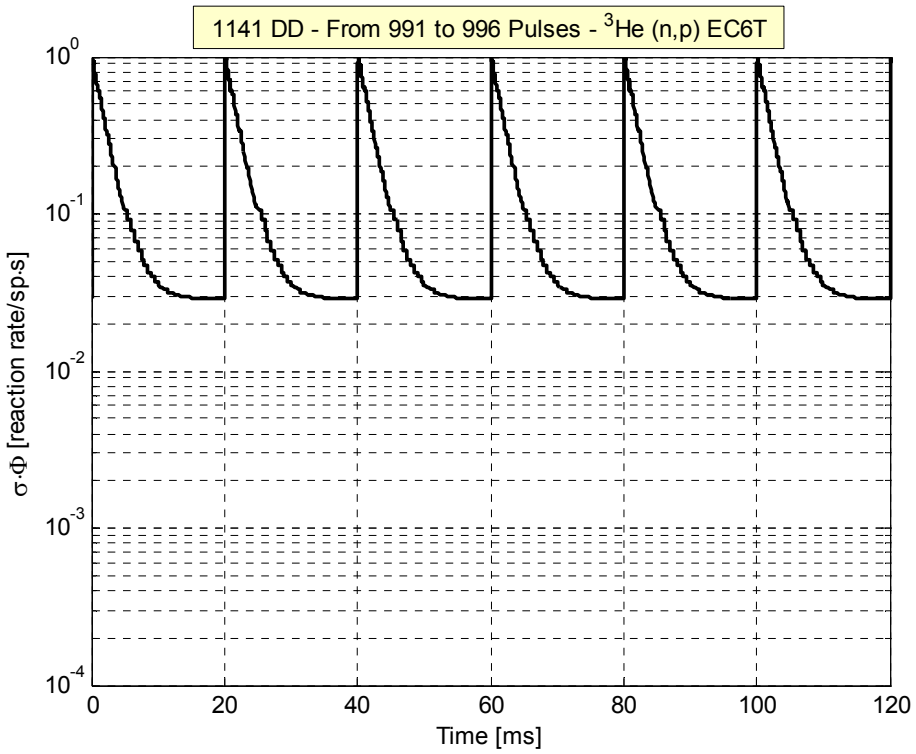

Figure 12. ^{3}He(n,p) reaction rate calculated for 6 successive D-D neutron pulses starting from pulse number 991 for the 1141 YALINA-Booster configuration

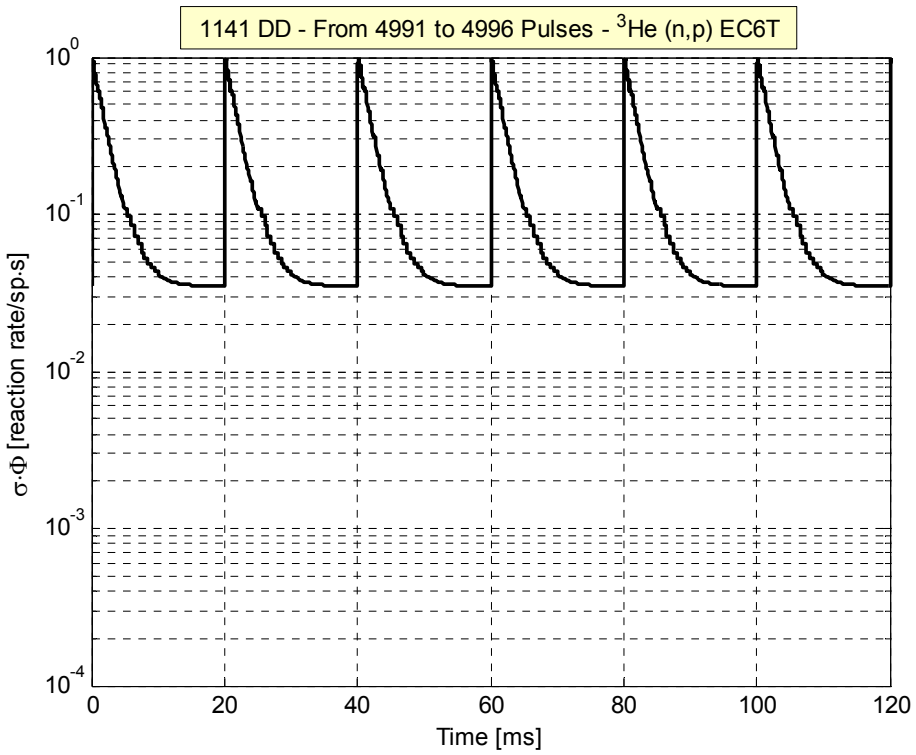

Figure 13. ^{3}He(n,p) reaction rate calculated for 6 successive D-D neutron pulses starting from pulse number 4991 for the 1141 YALINA-Booster configuration

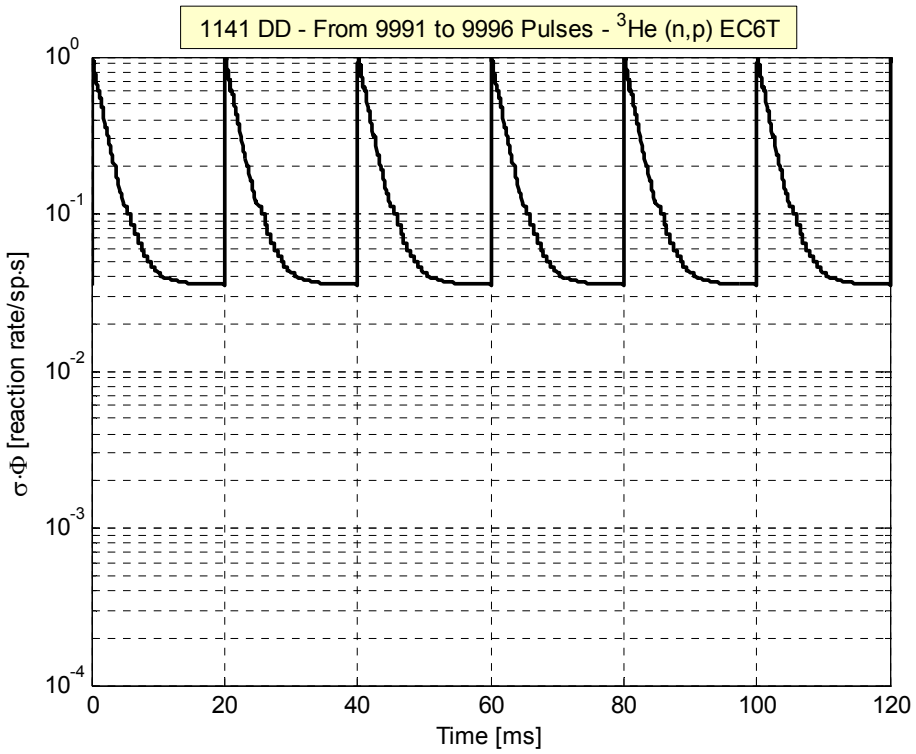

Figure 14. ^{3}He(n,p) reaction rate calculated for 6 successive D-D neutron pulses starting from pulse number 9991 for the 1141 YALINA-Booster configuration

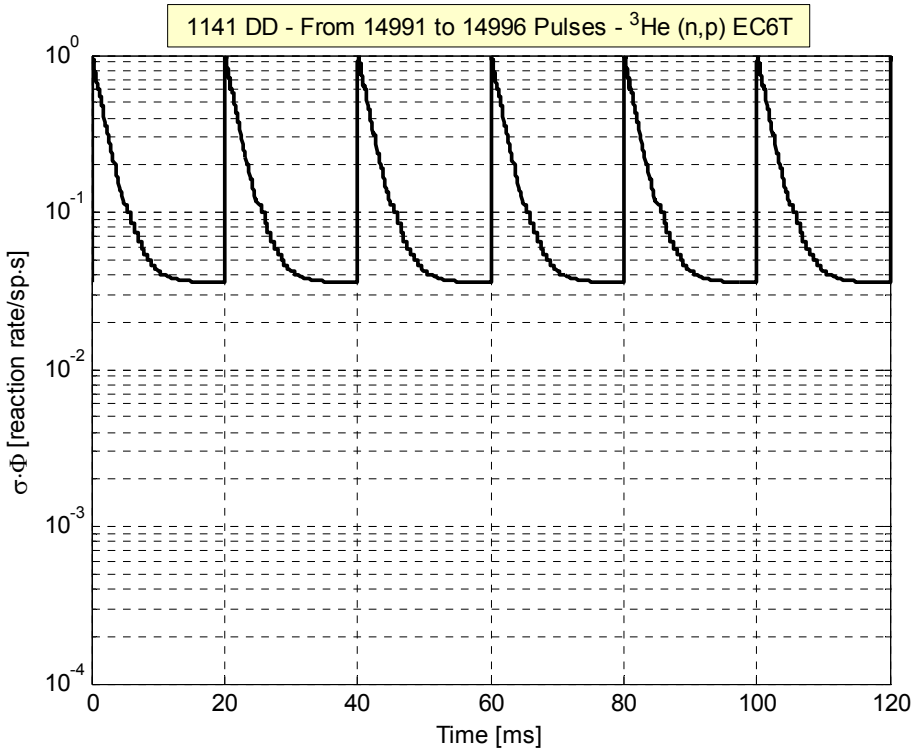

Figure 15. ^{3}He(n,p) reaction rate calculated for 6 successive D-D neutron pulses starting from pulse number 14991 for the 1141 YALINA-Booster configuration

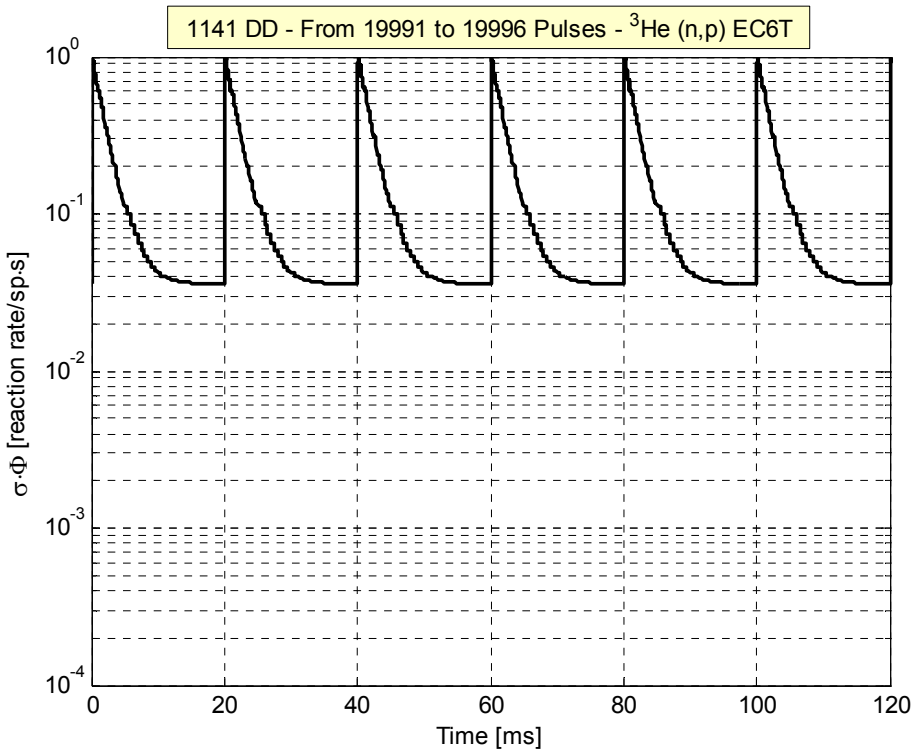

Figure 16. ^{3}He(n,p) reaction rate calculated for 6 successive D-D neutron pulses starting from pulse number 19991 for the 1141 YALINA-Booster configuration

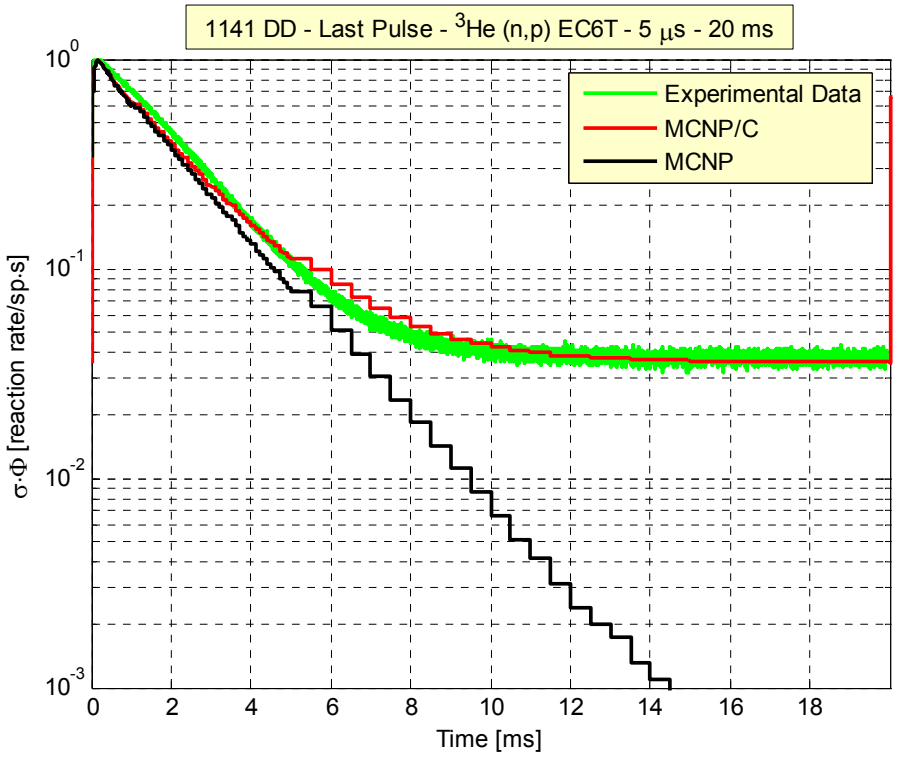

Figure 17. ^{3}He (n,p) reaction rate in EC6T experimental channel of the 1141 YALINA-Booster configuration for the last D-D neutron pulse

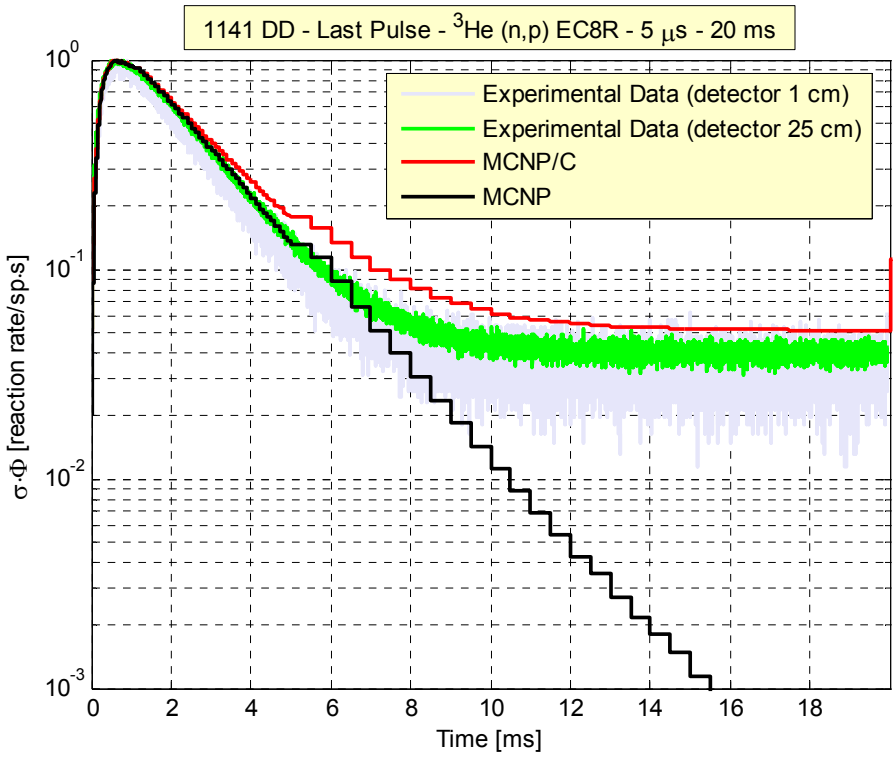

Figure 18. ^{3}He (n,p) reaction rate in EC8R experimental channel of the 1141 YALINA-Booster configuration for the last D-D neutron pulse

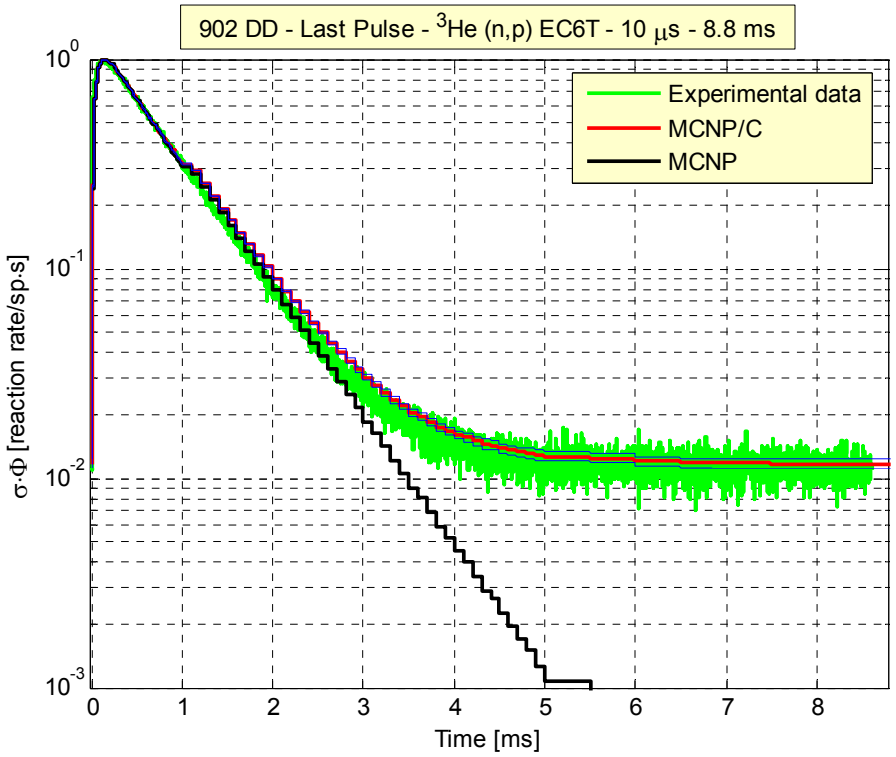

Figure 19. ^{3}He (n,p) reaction rate in EC6T experimental channel of the 902 YALINA-Booster configuration for the last D-D neutron pulse

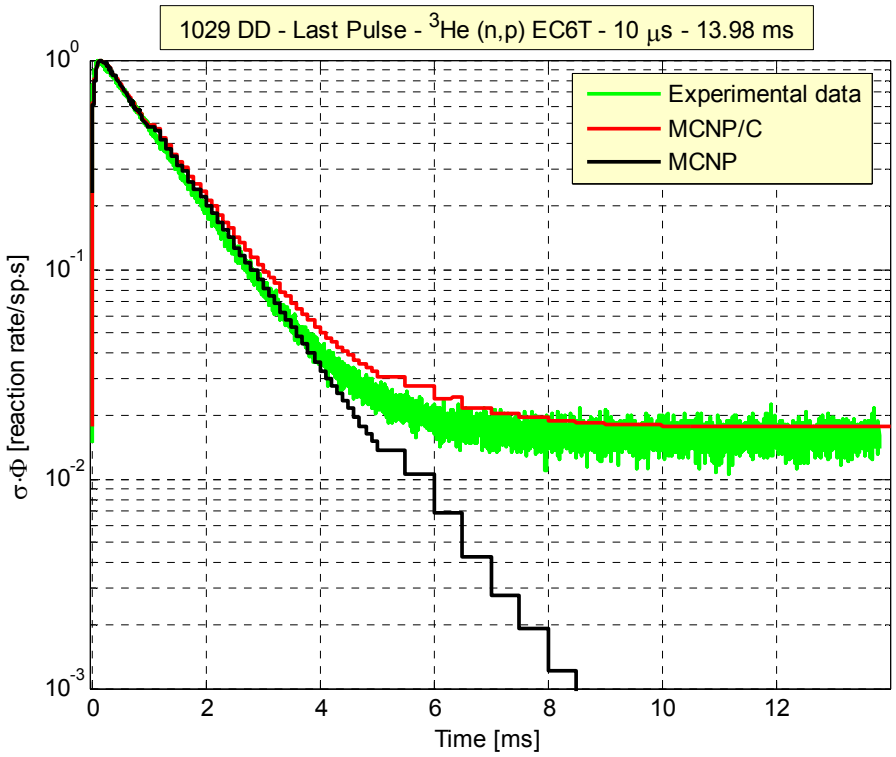

Figure 20. ^{3}He (n,p) reaction rate in EC6T experimental channel of the 1029 YALINA-Booster configuration for the last D-D neutron pulse

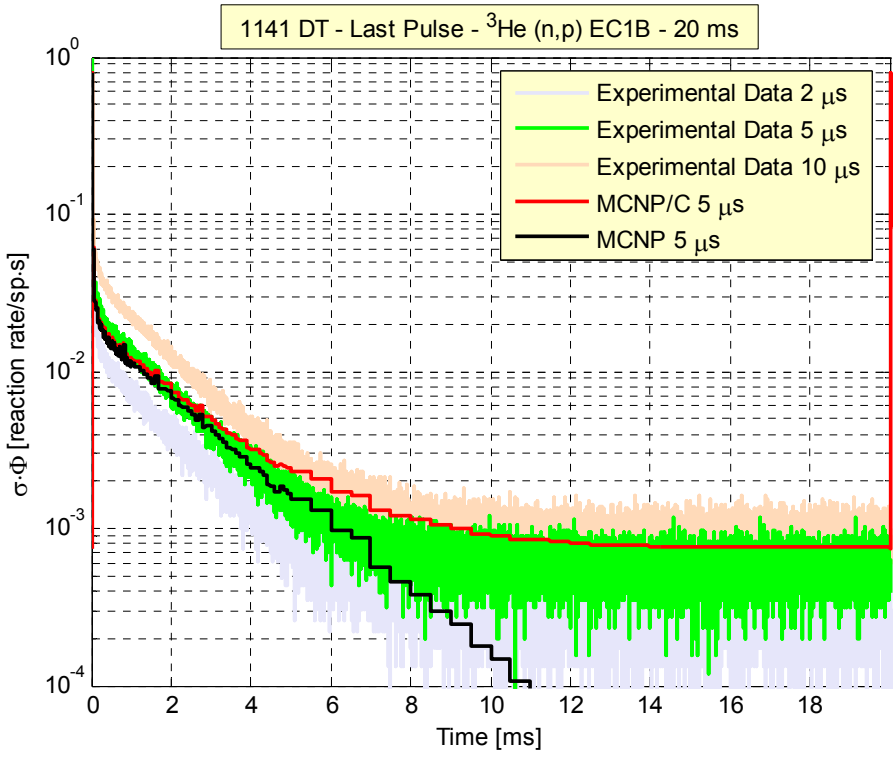

Figure 21. ^{3}He (n,p) reaction rate in EC1B experimental channel of the 1141 YALINA-Booster configuration for the last D-T neutron pulse

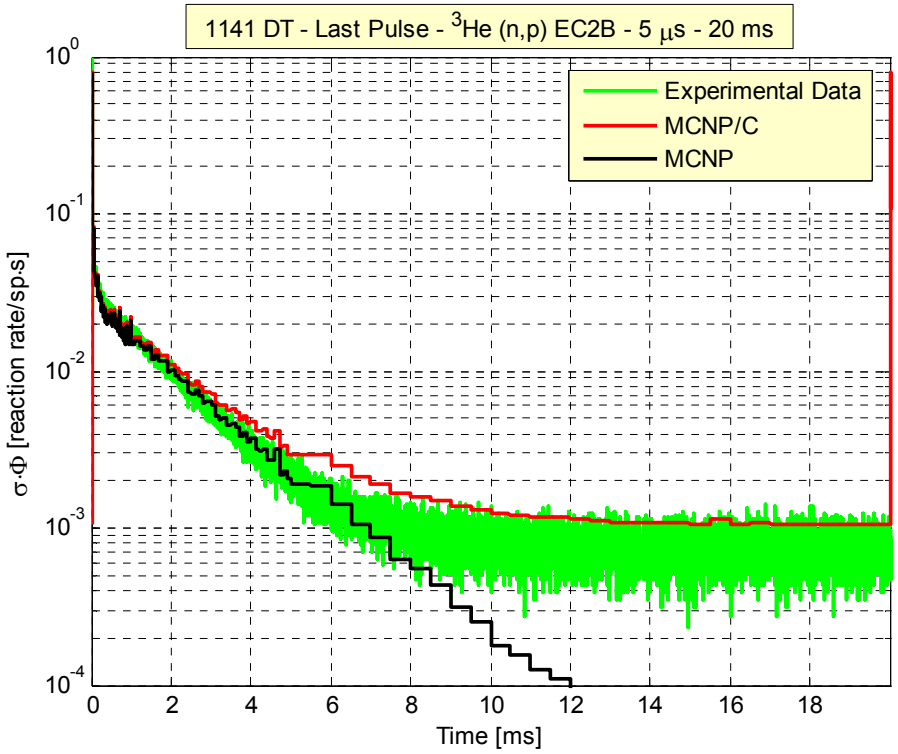

Figure 22. ^{3}He (n,p) reaction rate in EC2B experimental channel of the 1141 YALINA-Booster configuration for the last D-T neutron pulse

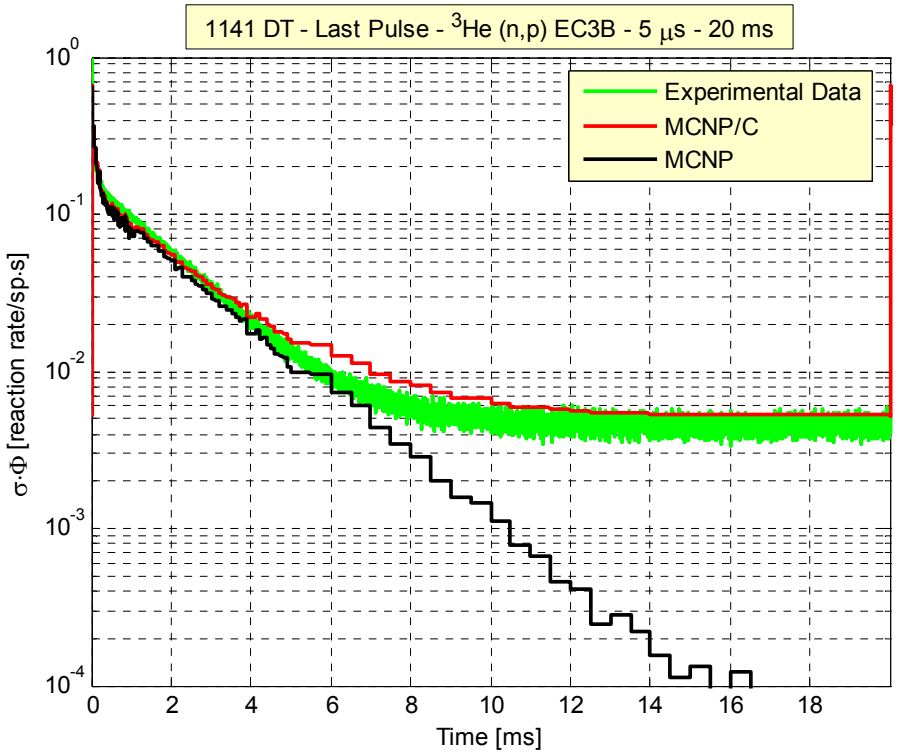

Figure 23. ^{3}He (n,p) reaction rate in EC3B experimental channel of the 1141 YALINA-Booster configuration for the last D-T neutron pulse

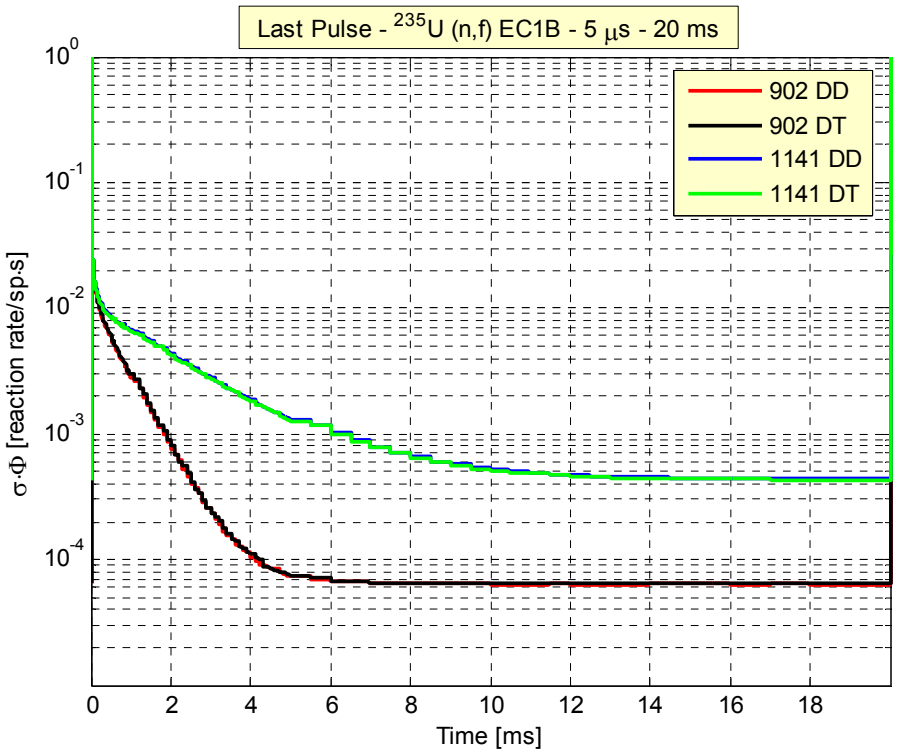

Figure 24. ^{235}U fission reaction rate reaction rate in EC1B experimental channel of the YALINA-Booster configuration for the last neutron pulse

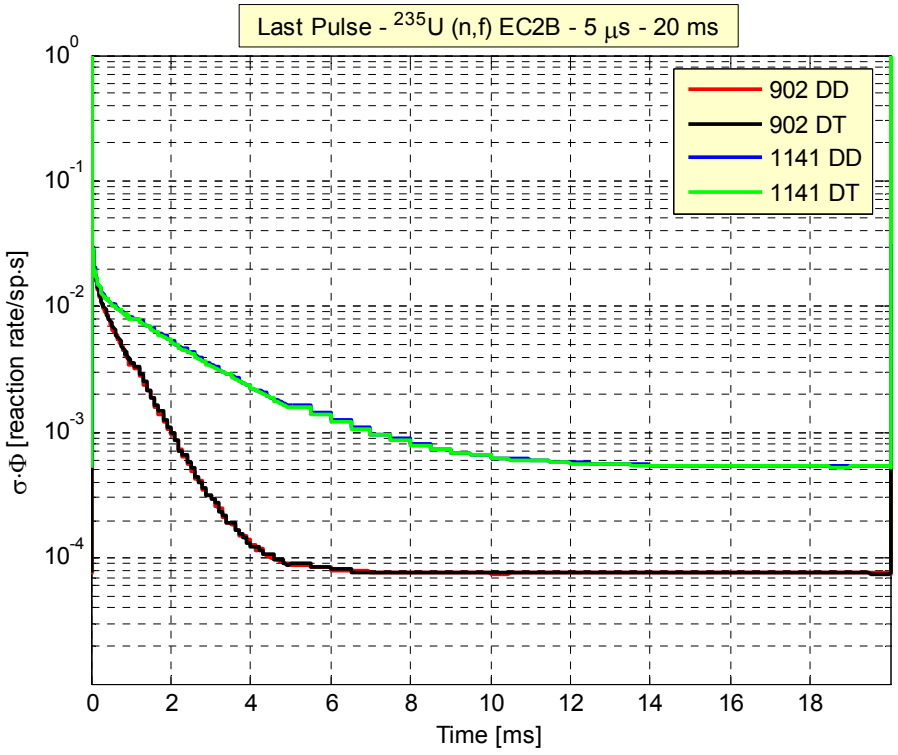

Figure 25. ^{235}U fission reaction rate reaction rate in EC2B experimental channel of the YALINA-Booster configuration for the last neutron pulse

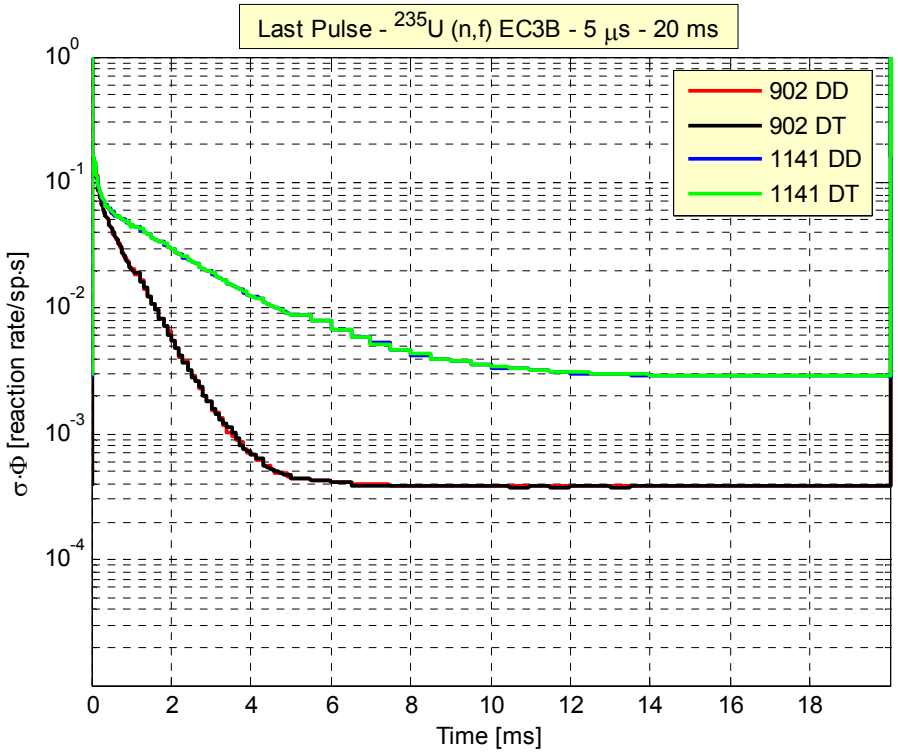

Figure 26. ^{235}U fission reaction rate reaction rate in EC3B experimental channel of the 1141 YALINA-Booster configuration for the last neutron pulse

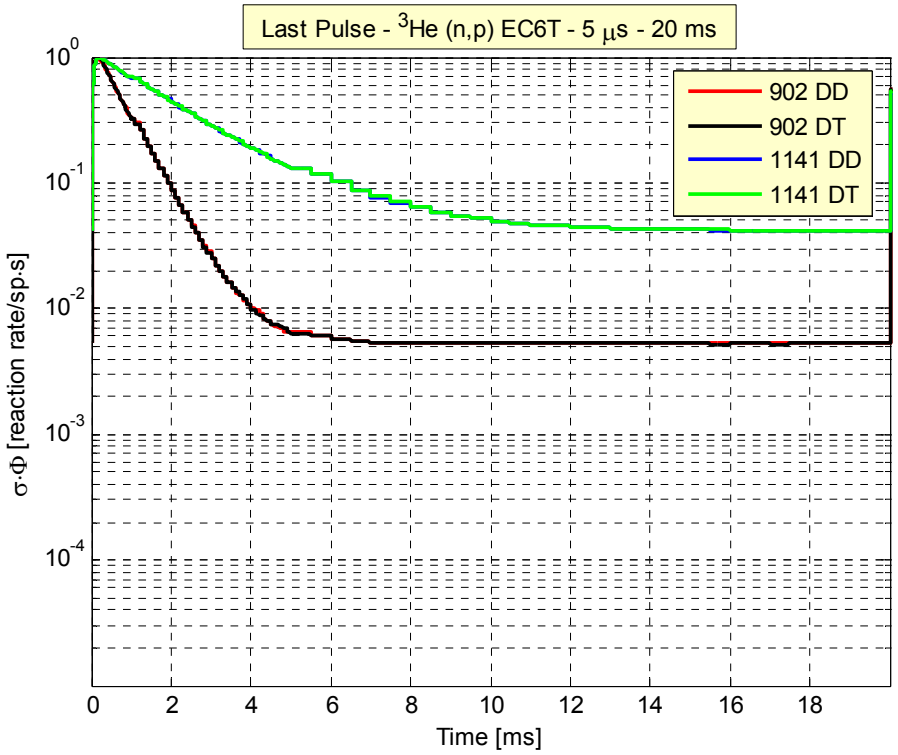

Figure 27. ^{3}He (n,p) reaction rate reaction rate in EC6T experimental channel of the YALINA-Booster configuration for the last neutron pulse

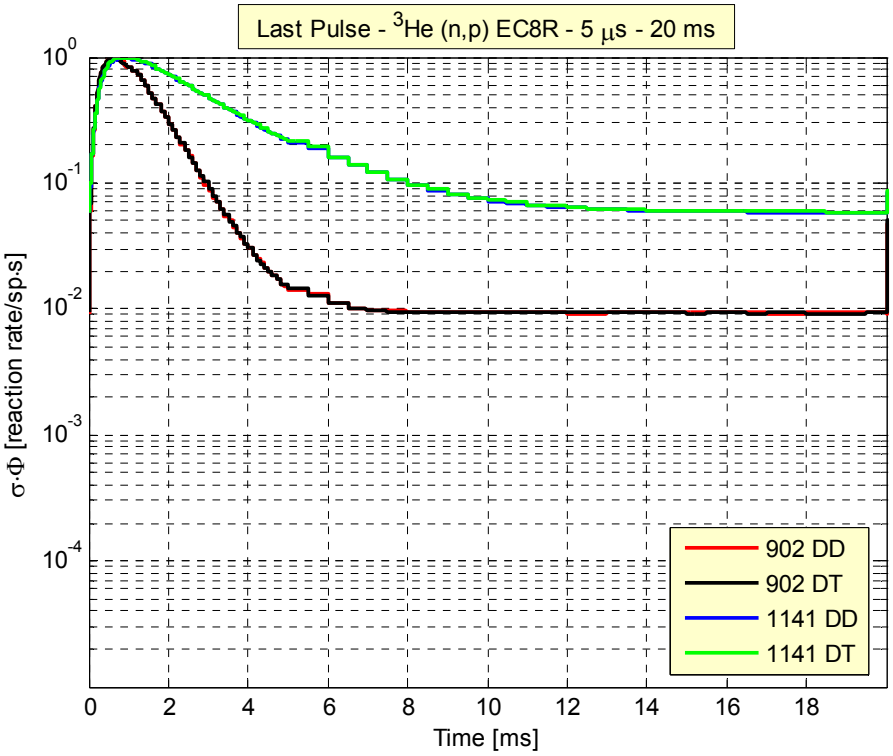

Figure 28. ^{3}He (n,p) reaction rate in EC8R experimental channel of the YALINA-Booster configuration for the last neutron pulse

Nuclear Engineering Division
Argonne National Laboratory
9700 South Cass Avenue, Bldg. 208
Argonne, IL 60439-4842

www.anl.gov

A U.S. Department of Energy laboratory managed by UChicago Argonne, LLC